Sensors & Actuators: B. Chemical 425 (2025) 136960

Contents lists available at ScienceDirect

Sensors and Actuators: B. Chemical

journal homepage: www.elsevier.com/locate/snb

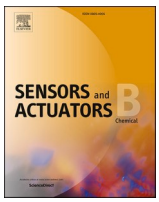

Wide range luminescence lifetime-based pH sensing with covalently immobilized multi-protonatable Ru(II) complexes

Ya Jie Knöbl [a], Maximino Bedoya [a,1], Alexander Farquharson [a], Patrick Courtney [b,2], Guillermo Orellana [a,*]

[a] Optical Chemosensors & Applied Photochemistry Group (GSOLFA), Dpmt. of Organic Chemistry, Faculty of Chemistry, Complutense University of Madrid, Plaza de las Ciencias 2, Madrid 28040, Spain

[b] TAP Biosystems (currently Sartorius Stedim TAP), Grantham Cl, York Way, Royston SG8 5WY, UK

ARTICLE INFO

Keywords:
pH sensor
Luminescence
Emission lifetime
Phase-sensitive detection
Ruthenium polypyridyl complexes
Fermentation monitoring

ABSTRACT

To overcome the limitations of optical pH sensors, the response of which is just ca. one pH unit around the pK_a value of the indicator dye and capitalize on the advantages of red-luminescent Ru(II) complexes for optical sensing, multi-pK_a members of this family are proposed. Bipyridine ligands bearing protonatable groups (amines and carboxylates) are the basis to design and prepare the indicator dyes. Their photophysical properties and response to pH changes were investigated in the pH 3.5 – 9.0 range. The complex [Ru(DCB)$_2$DEAMB], where DCB and DEAMB stand for 2,2'-bipyridine-4,4'-dicarboxylate and 4,4'-(*N,N*-diethylaminomethyl)-2,2'-bipyridine, respectively, shows a reversible monotonic change of its emission wavelength maximum (648 – 634 nm), luminescence intensity (1.40x) and lifetime (335 – 429 ns) in solution with increasing pH. This complex and two similar ones were covalently tethered to commercial TentaGel® M Br polymer microbeads for luminescence phase shift fiberoptic pH measurements. The immobilized [Ru(DCB)$_2$DEAMB] displays the widest pH sensitivity over pH 3.5 to pH 8.5. The stability of this sensor was satisfactory when cycling between pH 3.5 and 8.5 for five days as well as under a three-day cycle between each pH unit. Changes of the buffer type, buffer concentration and osmolarity did not significantly influence the sensor response; however, large variations of dissolved oxygen and, naturally, temperature would require correction by the corresponding sensors. The novel, robust luminescent pH sensor has been tested in phase-sensitive mode for cell cultures monitoring in commercial bioreactors, but its response would also be suitable for in situ monitoring of natural waters.

1. Introduction

For a streamlined process in a bioreactor, the monitoring of different biological, chemical and physical parameters is paramount. To this end, different sensors are deployed and measured in-line for precise readings [1]. Among these parameters, pH is an essential one and to measure it, the pH glass electrode is chosen so far because of its wide response (pH 0 – 13), accuracy (± 0.01 pH units), precision, and response time. Despite their evident usefulness, glass electrodes are fragile, difficult to miniaturize, expensive, and subject to rapid biofouling, contamination, and interferences from external equipment. All these effects can result in significant signal drift that requires frequent maintenance for the required sensor performance in cell culture monitoring [2,3].

For selected applications, optical-based pH sensors (also known as pH optodes) have gained popularity [4–6]. Using the working principle of colorimetric or fluorometric changes, such sensors are immune to electrical interference, can be miniaturized at low cost and are robust in hostile environments. While absorption or luminescence intensity-based sensors can be subject to non-specific changes due to excitation light fluctuations, detector drift or indicator dye leaching, emission lifetime-based sensors are self-referenced and therefore immune to most environmental effects. In addition, lifetime measurements can be conducted using phase-sensitive detection of the luminescence, thereby simplifying the complexity of the final measurement device, lowering manufacturing costs, and ultimately increasing the attractiveness of optical sensors based on luminescence lifetime measurement, as

* Corresponding author.
E-mail address: orellana@quim.ucm.es (G. Orellana).
[1] Present address: Equilab, S.A., Avda. Camino de lo Cortao, 21 – Nave 6, 28703 San Sebastián de los Reyes (Madrid), Spain
[2] Present address: tec-connection, neuwerk, Oberlohnstrasse 3, 78467 Konstanz, Germany

https://doi.org/10.1016/j.snb.2024.136960
Received 6 October 2024; Received in revised form 30 October 2024; Accepted 15 November 2024
Available online 19 November 2024

evidenced with the success of luminescent sensors for dissolved oxygen in water [7–9].

Despite all of the above advantages, typical indicator-based optical pH sensors are able to operate only within 1 – 1.5 pH units around their (ground or excited state) pK_a value, i.e. the region where they exhibit enough sensitivity [4]. To extend the measurement range, two different approaches can be used. The first one is to mix different indicator dyes with overlapping sensitivity ranges and a uniform response to pH changes [10–12]. However, since multi-dye sensors are based on absorbance or luminescence intensity measurements, they are subject to the limitations mentioned above. The second way to achieve an optical pH sensor with extended sensing range is to use a single indicator dye with multiple pK_a values, yet the known ones are also based on luminescence intensity measurements [13–15].

Dyes based on Ru(II) polyazaheteroaromatic complexes may be particularly suitable to this approach due to the possibility of ligand engineering to achieve tunable photophysical properties [16,17]. Furthermore, the large Stokes shift and satisfactory luminescence (quantum yield and lifetime) facilitate the design of sensing devices, and their excellent photochemical and thermal stability ensures the long-term use of sensors based on these indicator dyes. Acidity/pH sensors containing Ru(II) dyes reported so far utilize moieties such as carboxy, sulfonic, hydroxy, amine, pyridine or pyrazine on the polypyridyl ligands as the pH sensitive features [1,17–29].

However, it should be noted that not all ruthenium polypyridyl complexes are genuine pH indicator dyes. Orellana and co-workers have demonstrated that although most of those complexes show changes in their luminescence lifetime with pH, the variations are dependent on the buffer and its concentration used to set the pH value [19]. In that case, the response to acidity changes is due to competitive irreversible proton transfer to/from the luminescent triplet metal-to-ligand charge transfer (^{3}MLCT) excited state. In other words, a chemical equilibrium is not established within the lifetime of the protonated and deprotonated photoexcited indicator dye [30]. Such photoinduced proton transfer prevents the use of those pH-responsive ruthenium complexes as pH indicator dyes and restricts their use to acidic or alkaline gas monitoring (e.g. CO_2, NH_3…) [31,32] where the acidity/basicity of the internal indicator layer is carefully controlled [33].

In this work, a new family of heteroleptic ruthenium polypyridyl complexes has been designed and synthesized to be employed as wide range luminescent pH sensors for intensity and lifetime measurements. Starting with the 2,2′-bipyridine-4,4′-dicarboxylic acid (DCB) ligand and the corresponding bis-chelate complex $Ru(DCB)_2Cl_2$, complexes with various 4,4'-bis(aminomethyl)-2,2'-bipyridines have been obtained and their photophysical properties between pH 3.5 and 8.5 measured. The dependency on different buffers and their concentrations was evaluated to verify their applicability as true pH indicator dyes. The dyes are covalently immobilized on a solid polymer support and their characterization was performed to assess the effect of the solid support. Finally, the application of the widest range luminescent pH sensor to bioprocess monitoring using phase-sensitive measurement is shown [34].

2. Experimental section

2.1. Synthesis of the complexes

A scheme of the syntheses and structures of the target ligands and complexes is depicted in Fig. 1. Instrumentation, reagents, solvents, as well as full synthetic procedures are detailed in the Supporting Information.

2.2. Immobilization on the polymer support

Brominated cellulose has been prepared according to the literature [35] while the 10 µm brominated polymer beads (TentaGel® M-Br, abbreviated TGMB, capacity of 0.28 mmol g^{-1}) were purchased from Rapp Polymere (Tübingen, Germany). Briefly, cellulose is converted to allyl cellulose by refluxing powdered cellulose with allyl chloride before resuspending the cellulose in EtOH or water and adding dibromine.

An abbreviated procedure for covalent immobilization of the aminated indicator dye onto a brominated polymeric support is shown here while the detailed description is given in the SI. First, the brominated support is weighed into an Eppendorf tube and, together with an aqueous solution of the Ru(II) dye, the suspension is heated in an oven. Afterwards, the excess liquid is removed via centrifugation and washed until the supernatant becomes colorless. Then, a high pH buffer solution is added to the colored beads and the Eppendorf tube is placed again in the oven before the excess liquid is removed in the same way as before. The dyed beads are then dried and stored in the dark until use.

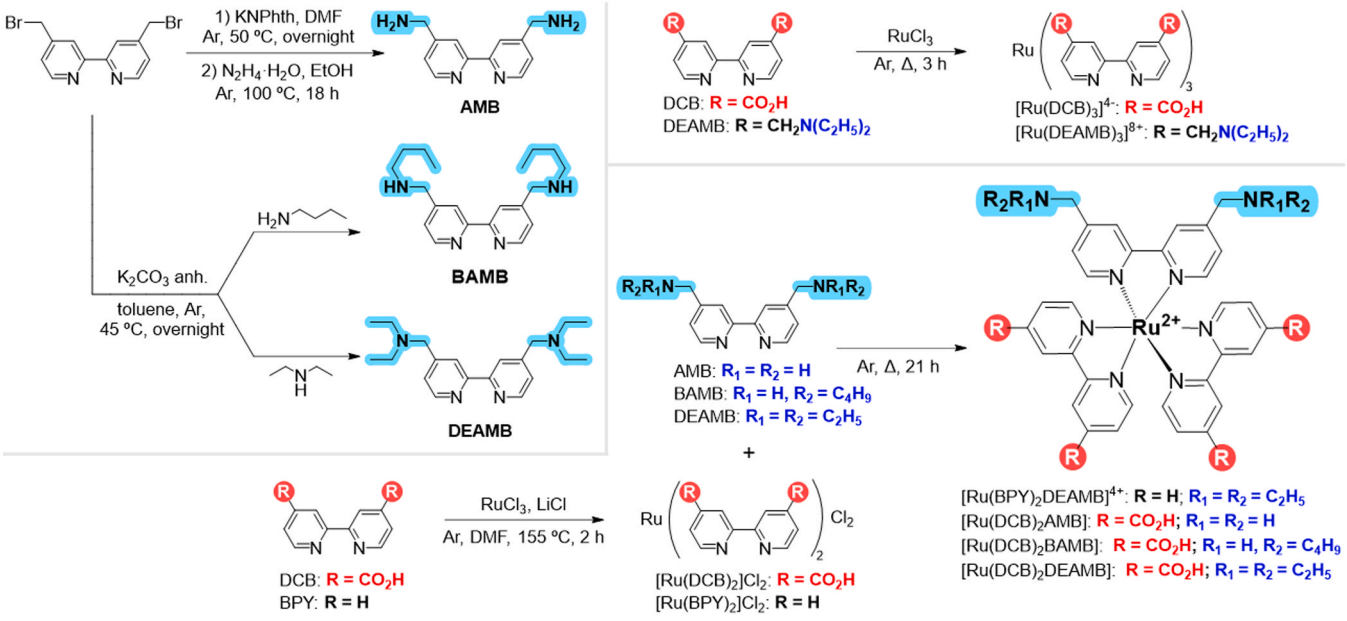

Fig. 1. A general scheme of the syntheses and structure of the prepared ligands and complexes. KNPhth: potassium phthalimide; DMF: *N,N*-dimethyl formamide; anh.: anhydrous.

2.3. Fabrication of pH sensor spots

Appropriate amounts of Polidisp® 2731 acrylic aqueous emulsion (Resiquímica, S.A., Porto, Portugal) and purified water (1:9 v/v) are thoroughly mixed. A 5 μL drop of the mixture is spread as a ca. 4 mm circle on 175 μm thick Mylar® (Goodfellow, USA) film and allowed to dry for 30 min at room temperature. Then, 10–20 μL of the dyed wet beads are mixed with 5 vol of purified water and vortexed. A 3 μL drop of the diluted dyed beads suspension is deposited, spread in an approximately 3 mm circle over the Polidisp adhesive and allowed to dry for 30 min at room temperature. A 4 mm disk filter (100 μm thick, 0.45 μm pore) of hydrophilic white polycarbonate film (Pall PolyPro GH, ref. 66340, New York, USA) is placed over the pH sensor spot as an opacifying layer. Finally, 5 mm disks are cut from the pH-sensitive spots to attach them to the corresponding sensor terminal (common end of the bifurcated optical fiber or inside the plastic bioreactor).

2.4. Preparation of buffer solutions

All buffer solutions (citrate, acetate, phosphate, bis-tris and borate) are either prepared by weighing a precise ratio of the acid and base forms of the buffer system or by mixing equimolar solutions of the acid and conjugate base of each buffer system. This ratio is calculated using the Henderson-Hasselbalch equation. A 200 mM concentration of KCl was also added to reproduce the conditions within bioreactors.

2.5. pH monitoring in a bioreactor

For the experiments in the test benchtop bioreactor, the ambr® 250 (TAP Biosystems, Royston, UK, currently Sartorius Stedium TAP) plastic culture vessel is used. The pH sensor spot is glued with a proprietary adhesive to the bottom of the vessel to be illuminated from the outside with the 525 nm LED of the optoelectronic unit through an optical fiber (see Supporting Information). Prior to any yeast culture experiment, the vessel is rinsed with 30 % H_2O_2 solution for sterilization and washed three times with water. Then, the vessel is placed into the ambr® 250 platform with the pH spot aligned to the optical fiber. A store-bought yeast in yeast extract peptone dextrose (YPD) media is placed inside and heated to 30 °C while an anaerobic environment is maintained throughout the run with N_2 gas.

3. Results and discussion

3.1. Selection of the ligands

As stated above, most pH indicator dyes based on Ru(II) complexes cannot be used as true indicator dyes owing to their dependency on the type and concentration of the buffer species used in the laboratory to achieve the desired pH value [19]. After careful study of the different pH-sensitive heterocyclic chelating ligands described so far, our selection was based on complementary pK_a values and their probability of being precursors of excited state acid-base equilibrium indicator dyes.

The DCB ligand was selected to provide the required sensitivity in the acidic region [36]. Nazeeruddin and Kalyanasundaram investigated heteroleptic Ru(II) complexes of bipyridine and DCB ligands with different substitution patterns in terms of their electronic state variations upon the pH changes [37]. According to their studies, the DCB ligand confers pH sensitivity to the complexes in both their absorption and luminescence based on the amount of DCB ligands introduced in the coordination sphere.

Regarding the sensitivity in the alkaline region, the aminomethyl group on the bipyridine ligand was chosen. Several authors have shown that heteroleptic complexes with 4,4'-*N,N*-diethylaminomethyl-2,2'-bipyridine (DEAMB) ligand and bipyridine (BPY) or diphenyl phenanthroline display a pK_a ~ 7.5 [38,39]. To take advantage of the effect of the degree and type of alkylation of the amine moiety on its sensitivity to pH, primary, secondary, and tertiary aminomethyl groups were tested while asymmetric ligands were not considered due to their more difficult synthesis and purification processes. Furthermore, care must be taken when the complexes with DCB or aminated bipyridine ligands are used in the synthesis as some sodium hydroxide has to be added to avoid ligand exchange and incomplete formation of the product.

3.2. Photophysical properties of the complexes

Heteroleptic [Ru(DCB)$_2$L] complexes, where L is 4,4′-*N,N*-diethylaminomethyl-2,2′-bipyridine (DEAMB), 4,4′-*N*-butylaminomethyl-2,2′-bipyridine (BAMB) or 4,4′-aminomethyl-2,2′-bipyridine (AMB) were synthesized. For the sake of comparison, [Ru(BPY)$_2$DEAMB]$^{4+}$ and the homoleptic complexes with DCB and DEAMB ligands were also synthesized. Overall charges of the discussed Ru(II) complexes are referred to their charges in pH 7 solutions (Fig. 2).

The absorption and emission spectra of all these complexes were measured at pH 3.5 and 8.5 in 50 mmol L^{-1} phosphate containing 200 mmol L^{-1} KCl, because these values represent the edges of the region of interest for the sought applications. The wavelength of the luminescence maximum and lifetime of each complex at low and high pH is shown in Table 1 while the full absorption and emission spectra of the complexes at pH 8.5 are shown in Fig. 2a. The Ru(II) dyes exhibit a broad band in the visible region (460 ± 15 nm) due to the d-π* transition to the ^{1}MLCT (metal-to-ligand charge transfer) excited state [16]. The bright orange-red emission around 650 nm and the long luminescence lifetime (> 200 ns) are also characteristic of the family of Ru(II) polypyridyl complexes.

Not surprisingly, the indicator dyes exhibit different luminescent features in acidic and basic solutions. Shorter emission lifetimes and lower intensities are observed in the former, accompanied by a bathochromic shift of the luminescence band. This may be explained by the energy gap rule, since the excited state of the acidic form of the complexes is more stable than that of the basic form, lowering the energy difference between the ground and excited states.

However, the homoleptic complex [Ru(DEAMB)$_3$]$^{8+}$ does not show the same behavior as all the other complexes. Instead of having a longer lifetime in alkaline media, it exhibits a shorter lifetime therein. To investigate this anomaly further, lifetime measurements were performed to see how the homoleptic and heteroleptic complexes behave within the pH range (Fig. 2b).

3.3. Effect of pH

The development of a wide range pH sensor requires a monotonic change of the emission lifetime within the sought range. Therefore, the emission lifetimes of the complexes were measured in the 3.5–8.5 pH range, set with 50 mmol L^{-1} phosphate buffer with 200 mmol L^{-1} KCl. Fig. 2b shows that only three of the synthesized complexes display such behavior, namely [Ru(DCB)$_3$]$^{4-}$, [Ru(BPY)$_2$DEAMB]$^{4+}$ and [Ru(DCB)$_2$DEAMB]. The observed plateau of the lifetime value of [Ru(DCB)$_3$]$^{4-}$ above pH 7 indicates that the fully deprotonated complex is formed. Protonation occurs upon decreasing pH, which leads to a shorter excited state lifetime due to the significant differences in the electronic features of DCBH$_2$ (CO_2H is a strong electron withdrawing substituent) vs. DCB (CO_2^- is neither a withdrawing nor donating substituent) [40]. On the other hand, [Ru(BPY)$_2$DEAMB]$^{4+}$ shows a monotonic lifetime increase only above pH 6.5 because it only contains basic –CH_2NR_2 moieties, with its behavior in agreement with a previous report [39]. The [Ru(DCB)$_2$DEAMB] indicator dye combines the behavior of both substituents and displays the sought monotonic variation of the luminescence lifetime between pH 4.0 and 8.5 (see below).

Replacement of the DEAMB ligand (a tertiary amine) with either AMB or BAMB, containing primary or secondary amino groups, respectively, does not increase the pH sensitivity range. Rather, these changes bring down the range where the lifetime changes are monotonic

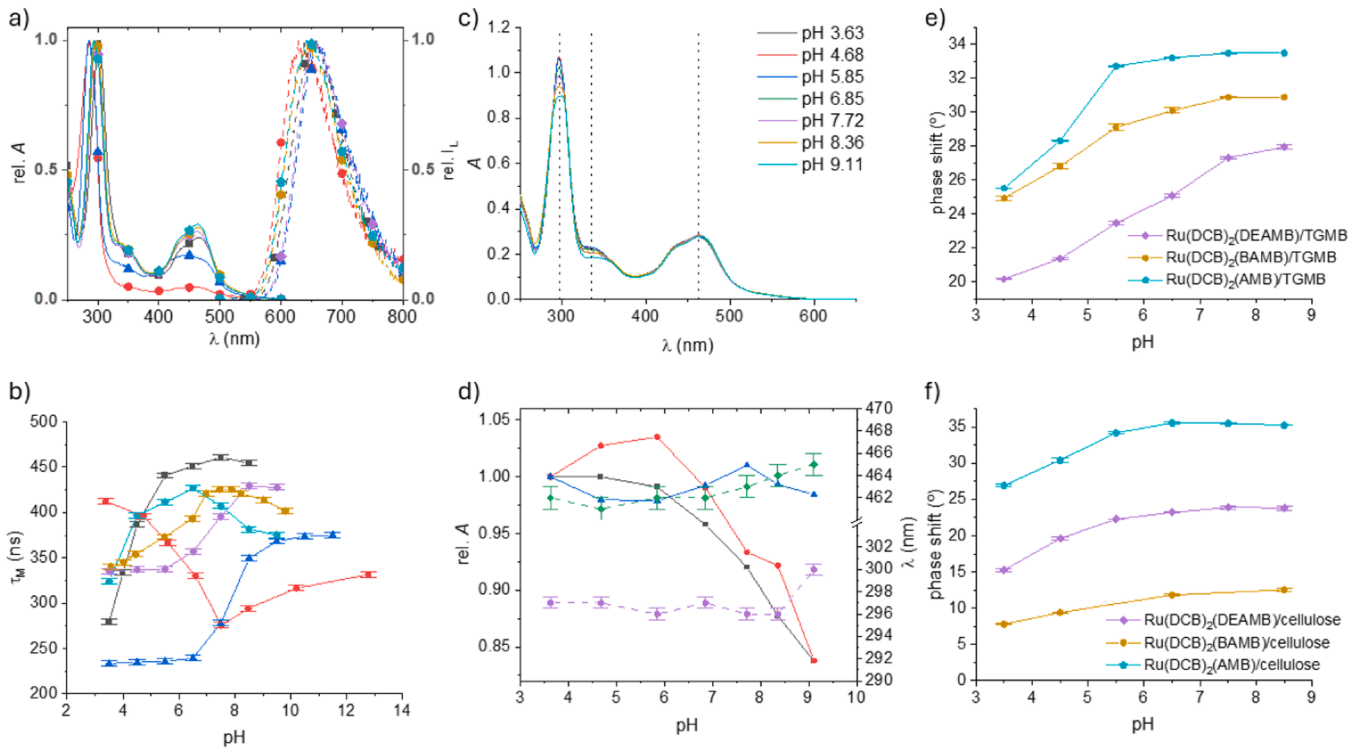

Fig. 2. $[Ru(DCB)_3]^{4-}$ (—■—), $[Ru(DEAMB)_3]^{8+}$ (—●—), $[Ru(BPY)_2DEAMB]^{4+}$ (—▲—), $[Ru(DCB)_2DEAMB]$ (—◆—), $[Ru(DCB)_2BAMB]$ (—⬢—), $[Ru(DCB)_2AMB]$ (—⬟—); **a)** Normalized absorption (—) and emission (— —) spectra recorded for the seven different complexes in 50 mmol L^{-1} pH 8.5 phosphate buffer containing 200 mmol L^{-1} KCl, emission collected using λ_{ex} = 465 nm. **b)** Luminescence lifetime of different complexes, measured in 50 mmol L^{-1} phosphate buffer containing 200 mmol L^{-1} KCl at different pH values under ambient conditions. **c)** Absorption spectrum of $[Ru(DCB)_2DEAMB]$ in 50 mmol L^{-1} phosphate buffer containing 200 mmol L^{-1} KCl as a function of pH. **d)** Changes of the relative absorbance at 297 nm (—■—), 335 nm (—●—) and 462 nm (—▲—) as a function of pH (the chosen maxima are depicted as dotted lines in Fig. 2c), and changes of the wavelength of the band maxima as a function of pH of $[Ru(DCB)_2DEAMB]$ in the UV (—◆—) and blue (—⬢—) region. **e)** Phase shift measurement of three complexes after immobilization on the commercially available solid support TentaGel® M-Br (TGMB). **f)** Phase shift measurement of three aminated complexes after immobilization on brominated cellulose. Uncertainty bars are calculated for $n = 3$.

Table 1
Parameters of the luminescence of the different Ru(II) dyes in 50 mmol L^{-1} phosphate buffer solutions containing 200 mmol L^{-1} KCl at (296 ± 2) K.[a]

Indicator dye	λ_{max} / nm		τ_M / ns	
	pH 3.63	pH 9.11	pH 3.63	pH 9.50
$[Ru(DCB)_2DEAMB]$	648	641	335	428
$[Ru(DCB)_2BAMB]$	648	637	341	407
$[Ru(DCB)_2AMB]$	642	643	324	427[b]
$[Ru(BPY)_2DEAMB]^{4+}$	658	628	233	368
$[Ru(DCB)_3]^{4-}$	658	629	279[c]	455
$[Ru(DEAMB)_3]^{8+}$	629	640[d]	412	276[d]

[a] The uncertainty values are ± 2 nm for the spectral maxima, 2 % for the emission lifetimes extracted from the best fit to biexponential functions ($I_L(t) = A_0 + \Sigma B_i \exp(-t/\tau_i)$). Preexponential weighted lifetimes ($\tau_M = \Sigma\tau_i B_i/\Sigma B_i$) have been measured in air.
[b] pH = 6.5
[c] The lifetime is 535 ns in Hammett acidity −1.06 (20 % H_2SO_4 by weight in water).
[d] pH = 7.5

(Fig. 2b), probably due to the lower basicity of the corresponding complexes. The homoleptic $[Ru(DEAMB)_3]^{8+}$ complex shows a longer lifetime in acidic medium (Table 1) as a consequence of the electron withdrawing character of the protonated methyl-*N,N*-diethylamino groups (+0.43 vs +0.01 for the $–CH_2NMe_2$, the only available values) [40]. Actually, full protonation of $[Ru(DCB)_3]^{4-}$ in strongly acidic medium also increases the lifetime of the deprotonated species (Table 1 footnote) due to the substituents effect (see above).

In an attempt to determine the individual ionization constants of the $[Ru(DCB)_2DEAMB]$ indicator dye, we measured the absorption spectra of the dye as a function of pH in phosphate buffer (Fig. 2c-d). Unfortunately, the spectra show very small variations of the absorbance with the pH changes. Furthermore, these changes and the wavelength shift of the spectral maxima are monotonous, and no plateaus are observed, thus preventing any calculation or estimation of the indicator ionization constants in the investigated range. We performed an analogous plot for the luminescence spectra (Fig. S1b-c in Supporting Information) with similar results.

3.4. Immobilization on polymer supports

In order to use the indicator dyes as luminescent pH sensors, they must be immobilized on a solid support, either covalently, electrostatically, or by simple inclusion into a matrix. While the use of a positively or negatively charged support for electrostatic immobilization would simplify fabrication, the additional solution ionic strength and the variation of the indicator overall charge with pH (see above) would wash out the dye from the support. Another option would be to incorporate the dye into a sol-gel matrix, a hydrogel, or other porous matrices, as it has been done for many other optical pH sensors [26, 41–44]. However, due to the high solubility of our complexes in water and the potential use of the sensors in bioprocess monitoring and watercourses, we decided to carry out a covalent attachment to the support to realize a robust immobilization of the indicator dye.

To that end, two different supports were chosen: brominated cellulose powder, and spherical beads consisting of a crosslinked poly(styrene) core and grafted ω-bromopoly(ethylene glycol) chains. Cellulose

was chosen for its water compatibility and its film-forming features, while the TGMB beads were chosen for its compatibility with all solvents, fast diffusion rate of waterborne species, and high degree of functionalization.

The selected indicator dyes for immobilization were the three heteroleptic complexes with varying degree of substitution on the aminomethyl moieties. The dyes were immobilized on the solid support by nucleophilic substitution of the terminal bromine atom, as shown schematically in Fig. 3a. Although the tertiary amine of the DEAMB ligand is a poor nucleophile, the excess of primary halide (around 20-fold) from the solid support and harsh conditions of the reaction (80 ºC for 24 h) should drive this reaction. After the covalent attachment, the solid support was heated in pH 11.5 phosphate buffer to remove ethylene from the DEAMB ligand in a Hofmann elimination. In this way, its pH sensitivity is restored by converting the immobilized quaternary alkylammonium back to a tertiary amine. In addition, the hydroxide ions convert any unreacted bromine into pH insensitive end groups (Fig. 3b and Supporting Information Fig. S2).

The pH sensitivity of the immobilized dyes in suspension was tested by measuring their luminescence lifetime as a function of pH in the 3.5 – 8.5 range before and after the final alkaline treatment (Supporting Information Figs. S3–4). Unlike the TGMB-immobilized complexes, the lifetime data of the cellulose-supported dyes show that the full pH sensitivity is not recovered until the final elimination step has been carried out. Nevertheless, the dyed cellulose powder performs less satisfactorily than the TGMB beads, probably due to the higher mobility of the grafted poly(ethylene glycol) chains at the distal end of which the attached amino group is placed compared to the brominated cellulose structure. Moreover, the response time of the TGMB-immobilized dyes is shorter than 4 s (Supporting Information Fig. S6).

Out of the three investigated complexes, the tertiary amine-substituted complex, namely [Ru(DCB)$_2$DEAMB]/TGMB, showed the best pH sensitivity in the range of interest, as seen in Fig. 2e. Therefore, this combination of dye and support was selected for further characterization.

3.5. pH response of the luminescent sensor

The selected beads were stuck to a PET window with the help of water-permeable acrylic glue (Fig. 3c-d). Then a thin, white, hydrophilic polycarbonate membrane was placed on top as a protective and reflective layer (see Supporting Information Fig. S7). The response function and the calibration curve of the sensor spots were determined (n = 7, Fig. 4a-b). Based on the response function in Fig. 4a, the average response time (t_{90}) is found to be ~12 min when the pH rises, and ~30 min when the pH decreases. Using our phase-sensitive optoelectronic interrogators [45], the sensitive spots show a dynamic range of 5 pH units (3.5 – 8.5) with a precision of ± 0.05 at pH 4.5 and pH 6.5, and ± 0.15 at pH 8.5 over 5 days (n = 7). Compared with other luminescent sensors that respond over a similar range [46–49], our sensor precision is on par or only slightly worse than those published in recent years (0.02 – 0.10 pH units). However, our sensor response times are longer than those reported (typically < 3 min). The rather long response times of our pH sensor are due to the 0.45 µm pore size overcoat polycarbonate membrane; additionally, the buffer addition and mixing times in the flow-through cell used for testing purposes might add to the sensor response time. In fact, removal of the overcoat or using the sensor in the wand-type mode reduces the response time to 30 and 180 s, respectively (Supporting Information Fig. S8). Nevertheless, the white overcoat produces a more efficient illumination of the supported pH indicator, yielding a higher s/n ratio.

Like all ruthenium polypyridyl complexes, the pH sensor is also sensitive to O_2 (Fig. 4c-d). Therefore, if the sensor application involves a large variation in the O_2 levels, the response should be corrected for all pH values. A similar real-time correction has been demonstrated for a luminescent Ru(II)-based sensor for ammonia monitoring [32].

The operational stability of the pH sensor was tested over 5 days upon pH 3.5/8.5 step changes (Fig. 4e) and was found to be better than

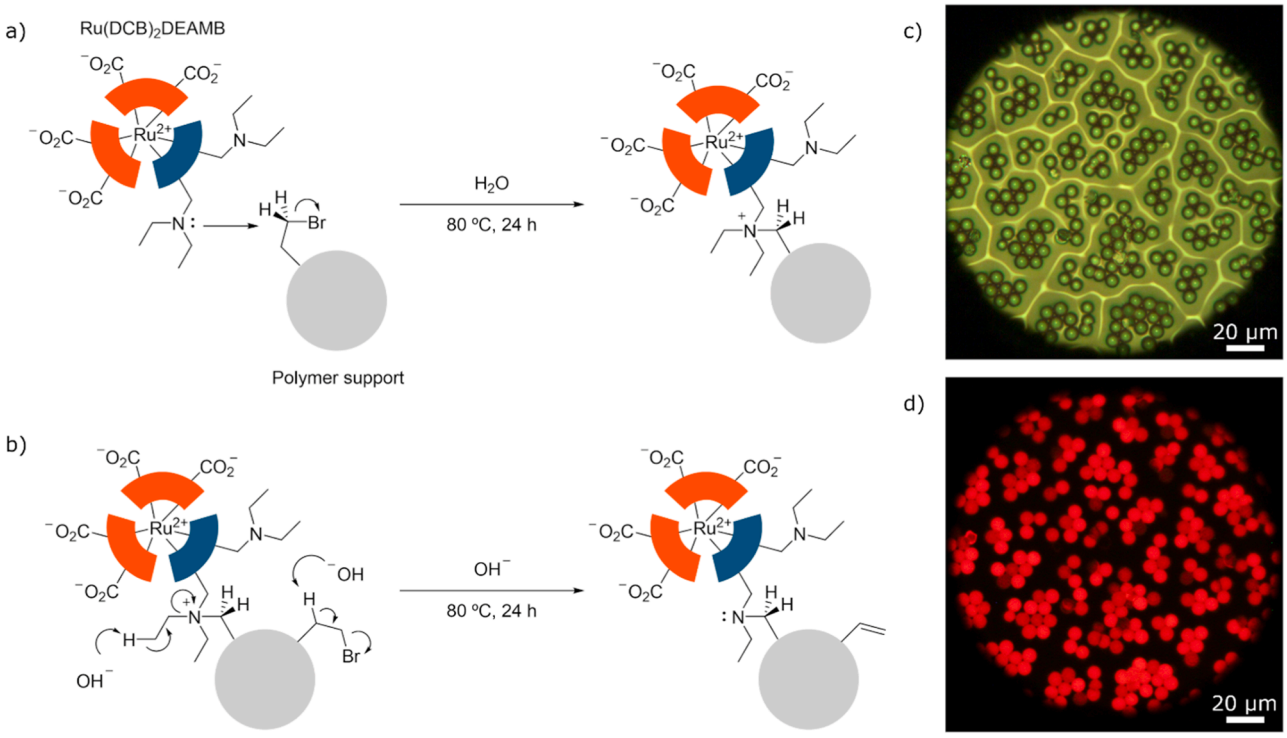

Fig. 3. a) Scheme of the covalent attachment of the selected indicator dye to the ω-brominated polymer beads (not to scale). **b)** Scheme of the suggested Hofmann elimination for improving the long-term stability of the dyed beads. **c)** Brightfield micrograph of [Ru(DCB)$_2$DEAMB]/TGMB glued to Mylar, without opacifier. **d)** Fluorescence micrograph of DEAMB/TGMB under the microscope; λ_{ex} = 463 nm.

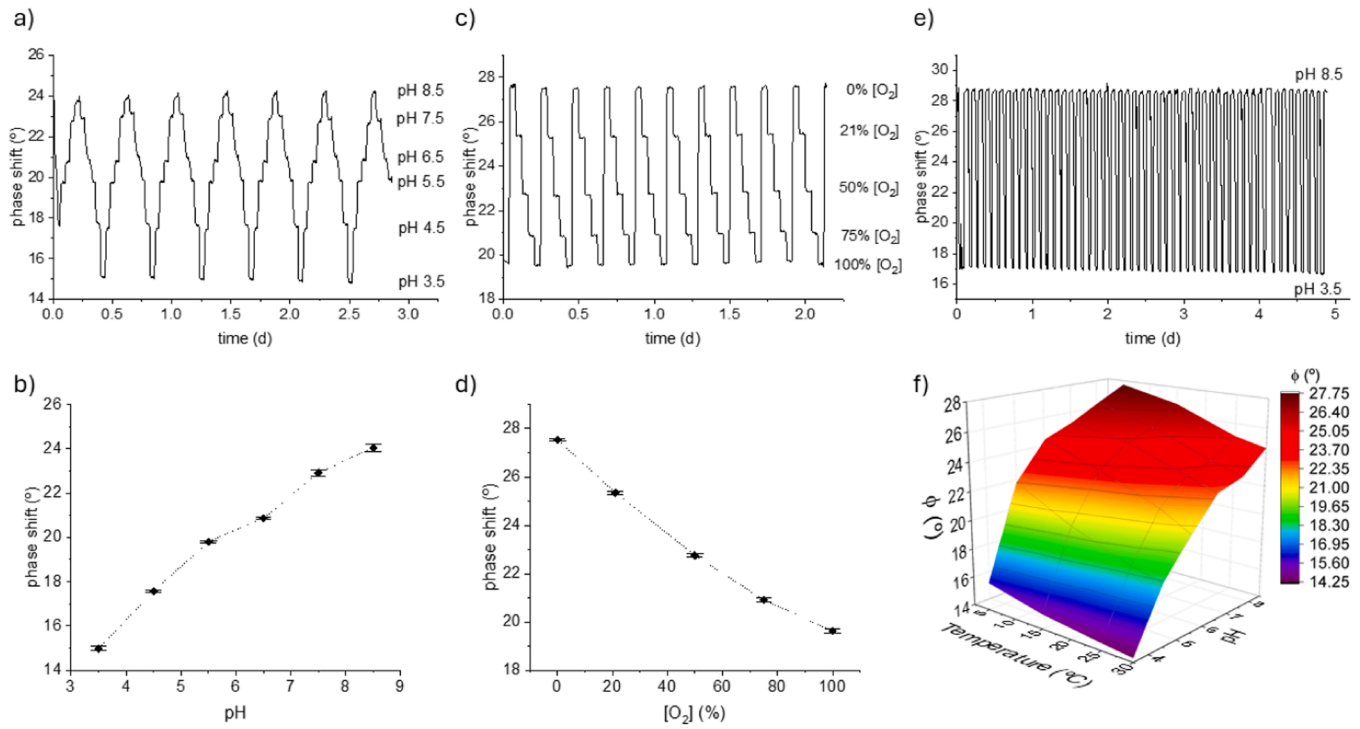

Fig. 4. a) Response function (pH 3.5–8.5 and back with intermediate steps of 1 pH unit in 50 mmol L^{-1} phosphate buffer with 200 mmol L^{-1} KCl) of the [Ru(DCB)$_2$DEAMB]/TGMB luminescent pH sensor at 25 °C, excited with a modulation frequency of 156 kHz. **b)** Calibration plot of the pH sensor from the data in Fig. 4a. Uncertainty bars are calculated for $n = 7$ (replicate measurements with the same sensor spot). **c)** Response function of the pH sensor to dissolved oxygen (as O_2% in a mixture with N_2) in pH 4.5 50 mmol L^{-1} phosphate buffer with 200 mmol L^{-1} KCl. **d)** Plot of pH sensor response to dissolved oxygen from the data in Fig. 4c. **e)** Stability of the pH sensor in air-equilibrated 50 mmol L^{-1} phosphate buffer with 200 mmol L^{-1} KCl at 25 °C. **f)** Temperature calibration of the dyed TGMB beads at 5, 15, 25 and 30 °C in the pH range 3.5 – 8.5 in aerated buffer solutions.

1 %. After storing the dry sensor spots in the dark at room temperature for six months, they provided the same response to pH variations. The sensor was also tested for its temperature effect (Fig. 4f). This effect mostly arises from the influence of the temperature on the excited state deactivation rate to the upper-lying non-emissive triplet metal-centered state from the luminescent ^{3}MLCT state of the Ru(II) complex [50].

3.6. Buffer type, concentration and ionic strength dependency

In order to confirm that the luminescent [Ru(DCB)$_2$DEAMB] complex is a true pH indicator dye, as discussed above, several tests with phosphate, citrate, borate, bis-tris and acetate buffers at various concentrations were performed (Fig. 5 and Supporting Information Fig. S10). The novel pH probe is not influenced by the nature of the buffer used to set the solution pH within the tested 3.5–9.5 range. Therefore, irreversible proton transfer quenching from the buffer is not involved in the deactivation of the excited state in that pH range [19,51,52].

As far as the buffer concentration is concerned, no difference of the indicator pH response was found in the investigated range. Only at 200 mmol L^{-1} phosphate the calibration curve slightly departs from the other tested concentrations due to the known ionic strength effect on charged indicator dyes. Luminescent intensity measurements corroborate these results (see Supporting Information Fig. S12).

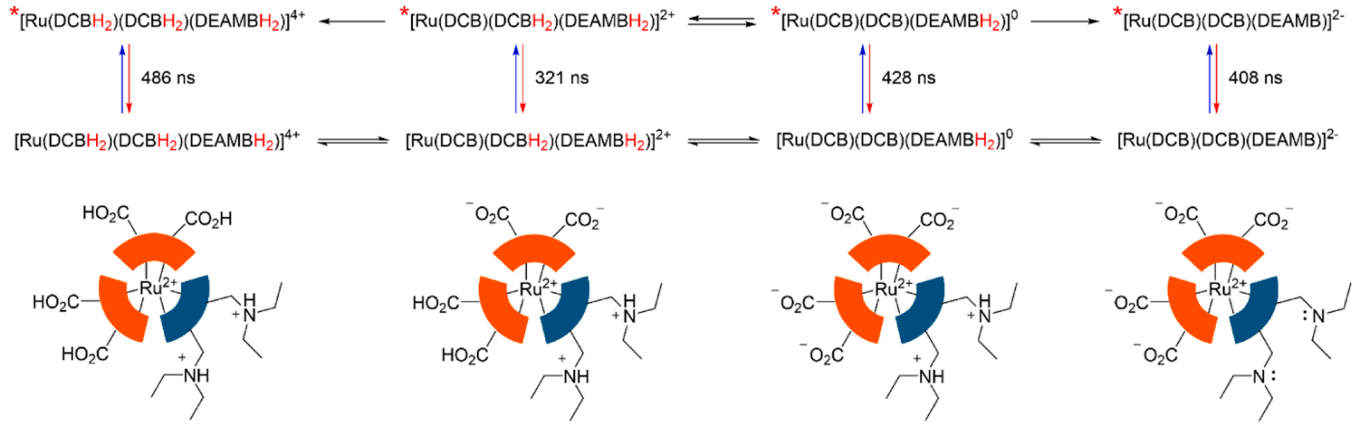

Fig. 5. Ground state equilibria and excited state proton transfer reactions that involve the [Ru(DCB)$_2$DEAMB] indicator dye in 50 mmol L^{-1} phosphate buffer containing 200 mmol L^{-1} KCl as a function of pH.

3.7. Luminescence lifetime as a function of pH

Due to the inability to determine the pK_a of the indicator dye from absorption and steady-state emission data, we analyzed the luminescence decays as a function of pH. Table 2 gathers the kinetic parameters extracted from the best fit with the least number of exponential functions to achieve a $\chi^2 < 1.20$. The percentages of the components represent the relative contribution of each species to the overall emission.

The emission measured at pH 10.3 follows a single-exponential decay ($\tau_1 = 408$ ns), corresponding to the emission of the fully deprotonated *[Ru(DCB^{2-})$_2$DEAMB]$^{2-}$ complex. Excited state proton transfer to this species or excited state equilibrium cannot occur as the concentration of Brönsted acids in the solution (H_3O^+ and protonated buffer or HB) at this pH value is negligible. As we lower the solution pH, the luminescent decay remains single exponential down to pH 8.0 ($\tau_2 = 429$ ns), even though the ground state protonation of the amine groups is progressively occurring. The two lifetimes are significantly different from each other (Table 2); therefore, the latter must correspond to the *[Ru(DCB^{2-})$_2$DEAMBH$_2^{2+}$]^0. Even though the lifetime values are different, the biexponential analysis is not able to resolve them because they are within 5 % of each other.

Below pH 8.0, we need an increasing contribution of a second exponential of a shorter lifetime to achieve successful fits of the luminescence decays. We have been able to use a global analysis of the decays from pH 7.5 to pH 4.0 to determine the individual lifetimes of the biexponential function ($\tau_2 = 428$ ns; $\tau_3 = 321$ ns; $\chi^2 = 1.247$). The shorter one should correspond to the *[Ru(DCB^{2-})(DCB**H$_2$**)DEAMB**H$_2^{2+}$**]$^{2+}$ indicator dye. The appearance of a double exponential indicates the lack of an excited state equilibrium; otherwise, we should observe a single exponential decay where the measured τ would be the weighted average of the lifetimes of the excited acid/base species [53,54]. Therefore, we have to conclude that the ground state equilibrium determines the relative contribution of the photoexcited acid/base forms, which do not interconvert within their lifetimes [19]. Furthermore, we have assumed so far that double (de)protonation takes place at every step as there is no evidence of intermediate inflection points [37,55]. Regarding the successive protonation of the DCB ligands, we have followed Nazeeruddin and Kalyanasundaram's studies on [Ru(DCB)$_2$BPY] which suggest that stepwise protonation of the Ru-coordinated DCB moieties occurs first on one ligand [37].

At pH 3.5, the decay remains biexponential but while τ_3 is still valid, we need to introduce a longer lifetime ($\tau_4 = 486$ ns) to get an acceptable fit. This is further confirmed by the luminescence decay measurement at pH 1.6, where the fit becomes single exponential, suggesting we are in the presence of the fully protonated photoexcited species that does not deprotonate within its lifetime. This is similar to the behavior observed for the fully deprotonated indicator dye. All the changes of the prevalent species as a function of pH discussed above are summarized in Fig. 5.

Table 2
Fitted lifetimes of the [Ru(DCB)$_2$DEAMB] indicator dye in 50 mmol L^{-1} phosphate buffer containing 200 mmol L^{-1} KCl at selected pH values with their individual contributions.[a]

pH	τ_1 (ns)	%	τ_2 (ns)	%	τ_3 (ns)	%	τ_4 (ns)	%
10.3	408	100						
9.5			428	100				
8.5			429	100				
8.0			429	100				
7.5			428	74	321	26		
7.0			428	66	321	34		
6.5			428	38	321	62		
6.0			428	35	321	65		
5.5			428	22	321	78		
5.0			428	28	321	72		
4.5			428	22	321	78		
4.0			428	21	321	79		
3.5					321	82	486	18
1.6							486	100

[a] The χ^2 of the global fit is < 1.35; the χ^2 of the individual fits is < 1.10.

4. In situ testing of the luminescent pH sensor

The performance of the luminescent pH microsensors was tested in a bioreactor with yeast culture with a pH electrode as a control. The ambr® 250 is a bioreactor system for fermentation or cell culture using single-use plastic culture vessels controlled by an automated workstation (Fig. 6b). After initial equilibration of the sensor spot in buffer media, the yeast broth is placed into the culture vessel, which also has sensors for dissolved oxygen (DO, luminescent), pH (amperometric) and temperature (thermocouple) monitoring, and two cultures were consecutively carried out (Fig. 6a). After each run, the vessel was taken out, the culture media was removed, and the vessel rinsed with water before placing the yeast broth again. It can be observed that the luminescent pH sensor readings closely follow the response of the pH electrode (Fig. 6a insets), but the former displays a more sluggish behavior (ca. 2 – 3 min delay). The pH sensor spot was not calibrated in situ but the calibration from another spot of the same batch was used; therefore, a small offset was to be expected. Further tests under different DO levels, temperature changes or interference from fluorophores are needed to verify the luminescent pH sensor usability under more complex situations. However, we have demonstrated that the sensor is able to meet the requirements of a pH sensor for actual culture systems and may be a substitute in the future for the traditional pH glass electrodes.

5. Conclusions

Thanks to the preparation of a novel family of ruthenium(II) polypyridyl complexes containing multi-protonatable sites, new wide-range pH indicator dyes for both steady-state and time-resolved luminescent sensing have been realized. The pH sensitivity of the dyes in solution increases when covalently attached to micrometer beads. Out of the designed dyes, the [Ru(DCB)$_2$DEAMB] complex shows the widest pH response (3.5 – 8.5). Despite the oxygen sensitivity, the luminescent sensor has been successfully used to monitor cell growth in bioreactors using the lifetime-based mode with phase shift interrogation. The developed sensor would also be useful to replace the glass electrode in surface water monitoring stations using the technology already commercialized for the luminescent sensing of dissolved oxygen. In this regard, further work is currently undertaken to test the wide-range pH sensor in combination with a luminescent O_2 sensor for this in situ application.

CRediT authorship contribution statement

Alexander Farquharson: Investigation. **Maximino Bedoya:** Validation, Methodology, Investigation, Formal analysis, Data curation, Conceptualization. **Guillermo Orellana:** Writing – review & editing, Validation, Supervision, Project administration, Methodology, Investigation, Funding acquisition, Formal analysis, Conceptualization. **Patrick Courtney:** Writing – original draft, Investigation, Data curation, Conceptualization. **Ya Jie Knöbl:** Writing – review & editing, Writing – original draft, Visualization, Investigation, Data curation.

Declaration of Competing Interest

The authors declare the following financial interests/personal relationships which may be considered as potential competing interests: Guillermo Orellana reports financial support was provided by TAP Biosystems (currently Sartorius Stedium TAP). Patrick Courtney reports a relationship with TAP Biosystems (currently Sartorius Stedium TAP) that includes: employment. Guillermo Orellana was previously co-Editor-in-Chief of Sensors & Actuators B: Chem., and is co-Editor for

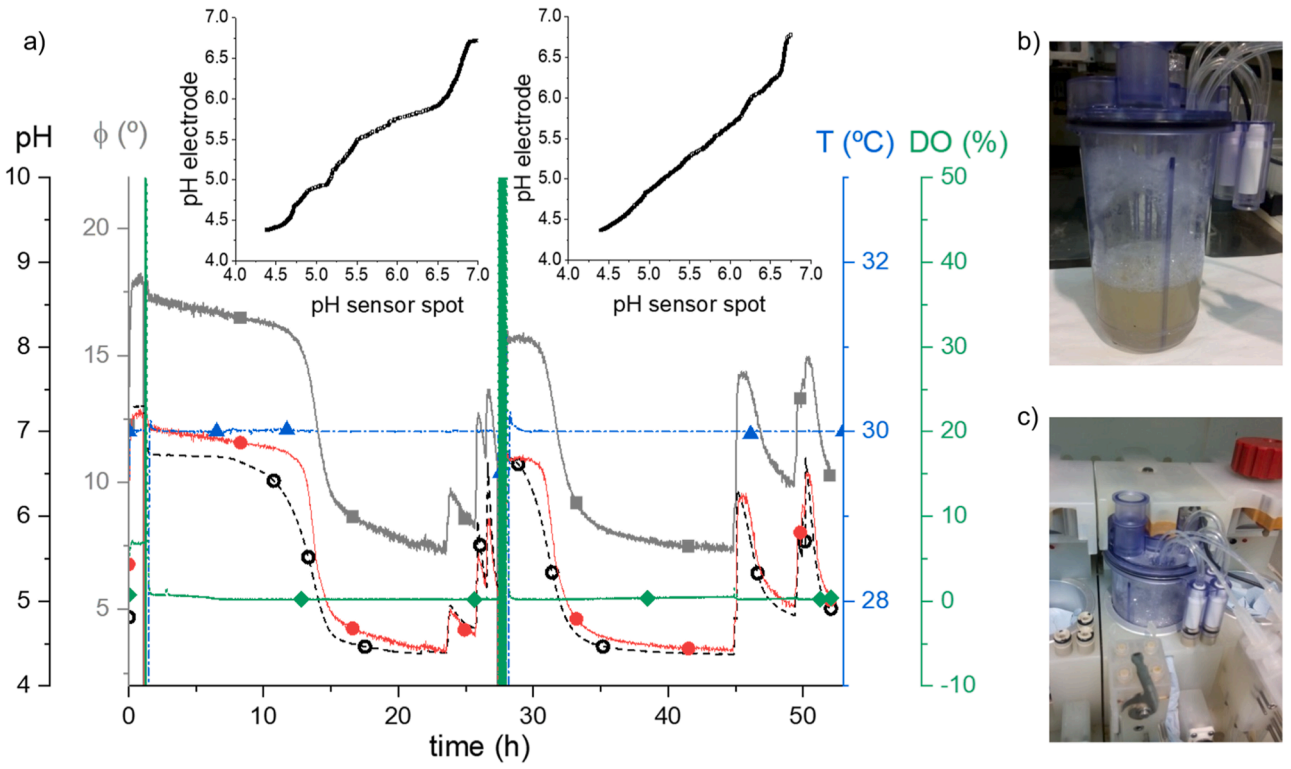

Fig. 6. a) Time-chart data obtained from anaerobic yeast cultures displaying the raw luminescence phase shift values (°, —■—), the luminescent pH sensor readings (—●—), the pH electrode measurements (—○—), the culture temperature (°C, —▲—), and dissolved oxygen (DO) levels (%, —) over two consecutive runs (bioreactor removal including rinsing and new culture addition occurring after ca. 27 h). The inset above each run depicts the correlation between the pH values measured with the luminescent pH sensor spot and with the pH electrode. **b)** Picture of the ambr® 250 plastic culture vessel after the first culture run. **c)** Picture of the ambr®250 platform with the vessel inside. The platform is connected via optical fibers (not shown) to the optoelectronic unit for the luminescent pH sensor measurements.

the VSI of Europtrode XVIII. Patrick Courtney was formerly an employee of TAP Biosystems (currently Sartorius Stedium TAP), but now has no relationship with his former employer. If there are other authors, they declare that they have no known competing financial interests or personal relationships that could have appeared to influence the work reported in this paper.

Acknowledgements

This project has been funded by TAP Biosystems (currently Sartorius Stedim TAP) under UCM contracts no. 324/2012, 223/2013 and 65/2014. The authors gratefully acknowledge the support for the work reported here, and permission for Fig. 6. YJK thanks UCM-FEI23/32–01 for a research fellow contract.

Appendix A. Supporting information

Supplementary data associated with this article can be found in the online version at doi:10.1016/j.snb.2024.136960.

Data availability

Data will be made available on request.

References

[1] I. Urriza-Arsuaga, G. Ielasi, M. Bedoya, G. Orellana, Luminescence-Based Sensors for Bioprocess Applications, in: B. Pedras (Ed.), Fluoresc. Ind., Springer International Publishing, Cham, 2019, pp. 1–38, https://doi.org/10.1007/4243_2019_10.

[2] K. Koren, C.M. McGraw, Let's talk about slime; or why biofouling needs more attention in sensor science, ACS Sens. (2023), https://doi.org/10.1021/acssensors.3c00961.

[3] K.F. Reardon, Practical monitoring technologies for cells and substrates in biomanufacturing, Curr. Opin. Biotechnol. 71 (2021) 225–230, https://doi.org/10.1016/j.copbio.2021.08.006.

[4] A. Steinegger, O.S. Wolfbeis, S.M. Borisov, Optical sensing and imaging of pH values: spectroscopies, materials, and applications, Chem. Rev. 120 (2020) 12357–12489, https://doi.org/10.1021/acs.chemrev.0c00451.

[5] P. Gruber, M.P.C. Marques, N. Szita, T. Mayr, Integration and application of optical chemical sensors in microbioreactors, Lab. Chip 17 (2017) 2693–2712, https://doi.org/10.1039/C7LC00538E.

[6] L. Li, A.V. Zhdanov, D.B. Papkovsky, Advanced multimodal solid-state optochemical pH and dual pH/O2 sensors for cell analysis, Sens. Actuators B Chem. 371 (2022) 132486, https://doi.org/10.1016/j.snb.2022.132486.

[7] J.R. Lakowicz, H. Szmacinski, Fluorescence lifetime-based sensing of pH, Ca2+, K+ and glucose, Sens. Actuators B Chem. 11 (1993) 133–143, https://doi.org/10.1016/0925-4005(93)85248-9.

[8] E. Kuwana, E.M. Sevick-Muraca, Fluorescence lifetime spectroscopy for pH sensing in scattering media, Anal. Chem. 75 (2003) 4325–4329, https://doi.org/10.1021/ac034059a.

[9] C. Huber, I. Klimant, C. Krause, O.S. Wolfbeis, Dual lifetime referencing as applied to a chloride optical sensor, Anal. Chem. 73 (2001) 2097–2103, https://doi.org/10.1021/ac9914364.

[10] R. Gotor, P. Ashokkumar, M. Hecht, K. Keil, K. Rurack, Optical pH sensor covering the range from pH 0–14 compatible with mobile-device readout and based on a set of rationally designed indicator dyes, Anal. Chem. 89 (2017) 8437–8444, https://doi.org/10.1021/acs.analchem.7b01903.

[11] J. Qi, D. Liu, X. Liu, S. Guan, F. Shi, H. Chang, H. He, G. Yang, Fluorescent pH sensors for broad-range pH measurement based on a single fluorophore, Anal. Chem. 87 (2015) 5897–5904, https://doi.org/10.1021/acs.analchem.5b00053.

[12] C. Carrillo-Carrion, W.J. Parak, Multiplexed fluorophore–nanoparticle hybrids for extending the range of pH measurements, Small Methods 1 (2017) 1700153, https://doi.org/10.1002/smtd.201700153.

[13] D.V. Snigur, A.N. Chebotarev, K.V. Bevziuk, Acid–base properties of azo dyes in solution studied using spectrophotometry and colorimetry, J. Appl. Spectrosc. 85 (2018) 21–26, https://doi.org/10.1007/s10812-018-0605-9.

[14] N.I. Georgiev, V.B. Bojinov, P.S. Nikolov, The design, synthesis and photophysical properties of two novel 1,8-naphthalimide fluorescent pH sensors based on PET

and ICT, Dyes Pigments 88 (2011) 350–357, https://doi.org/10.1016/j.dyepig.2010.08.004.
[15] J.J. Calmels, L. Aguilar, J. Mancebo-Aracil, G. Radivoy, C. Domini, M. Garrido, M. D. Sánchez, F. Nador, Novel pH-sensitive catechol dyes synthesised by a three component one-pot reaction, Front. Chem. 10 (2023) https://www.frontiersin.org/articles/10.3389/fchem.2022.1116887 (accessed July 14, 2023).
[16] G. Orellana, D. García-Fresnadillo, Environmental and Industrial Optosensing with Tailored Luminescent Ru(II) Polypyridyl Complexes, in: R. Narayanaswamy, O. S. Wolfbeis (Eds.), Opt. Sens. Ind. Environ. Diagn. Appl., Springer, Berlin, Heidelberg, 2004, pp. 309–357, https://doi.org/10.1007/978-3-662-09111-1_13.
[17] T. Mede, M. Jäger, U.S. Schubert, Chemistry-on-the-complex": functional Ru(II) polypyridyl-type sensitizers as divergent building blocks, Chem. Soc. Rev. 47 (2018) 7577–7627, https://doi.org/10.1039/C8CS00096D.
[18] M. Wu, Z. Zhang, J. Yong, P.M. Schenk, D. Tian, Z.P. Xu, R. Zhang, Determination and imaging of small biomolecules and ions using ruthenium(II) complex-based chemosensors, Top. Curr. Chem. 380 (2022) 29, https://doi.org/10.1007/s41061-022-00392-8.
[19] L. Tormo, N. Bustamante, G. Colmenarejo, G. Orellana, Can Luminescent Ru(II) Polypyridyl Dyes Measure pH Directly?, Anal. Chem. 82 (2010) 5195–5204. https://doi.org/10.1021/ac1005266..
[20] H.-J. Kim, Y.-C. Jeong, J. Heo, J.I. Rhee, K.-J. Hwang, A wide-range luminescent pH sensor based on ruthenium(II) complex, Bull. Korean Chem. Soc. 30 (2009) 539–540, https://doi.org/10.5012/bkcs.2009.30.3.539.
[21] B. Higgins, B.A. DeGraff, J.N. Demas, Luminescent transition metal complexes as sensors: structural effects on pH response, Inorg. Chem. 44 (2005) 6662–6669, https://doi.org/10.1021/ic050044e.
[22] W.J. Bowyer, W. Xu, J.N. Demas, Determining proton diffusion in polymer films by lifetimes of luminescent complexes measured in the frequency domain, Anal. Chem. 81 (2009) 378–384, https://doi.org/10.1021/ac8016554.
[23] H. Nam, M. Jeong, O.-J. Sohn, J.I. Rhee, J. Oh, Y. Kim, S. Lee, Synthesis of phenanthroline derivative by suzuki coupling reaction and the use of its ruthenium complex as an optical pH sensor, Inorg. Chem. Commun. 10 (2007) 195–198, https://doi.org/10.1016/j.inoche.2006.10.021.
[24] S. Kumar, S. Singh, A. Kumar, K.S.R. Murthy, A. Kumar Singh, pH-responsive luminescence sensing, photoredox catalysis and photodynamic applications of ruthenium(II) photosensitizers bearing imidazo[4,5-f][1,10]phenanthroline Scaffolds, Coord. Chem. Rev. 452 (2022) 214272, https://doi.org/10.1016/j.ccr.2021.214272.
[25] F. Gao, X. Chen, Q. Sun, J.-N. Cao, J.-Q. Lin, Q.-Z. Xian, L.-N. Ji, Boosting the sensitivity of pH responsible luminescent switches of polypyridyl ruthenium(II) complexes by structural design, Inorg. Chem. Commun. 16 (2012) 25–27, https://doi.org/10.1016/j.inoche.2011.11.021.
[26] Y. Clarke, W. Xu, J.N. Demas, B.A. DeGraff, Lifetime-based pH sensor system based on a polymer-supported ruthenium(II) complex, Anal. Chem. 72 (2000) 3468–3475, https://doi.org/10.1021/ac000111g.
[27] Z.-B. Zheng, S.-Y. Kang, Y. Zhao, N. Zhang, X. Yi, K.-Z. Wang, pH and copper ion luminescence on/off sensing by a dipyrazinylpyridine-appended ruthenium complex, Sens. Actuators B Chem. 221 (2015) 614–624, https://doi.org/10.1016/j.snb.2015.06.124.
[28] H. Yu, Z. Hao, H. Peng, R. Rao, M. Sun, R. Alana W, C. Ran, H. Chao, L. Yu, Near-infrared lysosome pH tracker and naked-eye colorimetric nucleic acids sensor based on ruthenium complexes [Ru(bim)2(dppz)]2+ and [Ru(bim)2(pip)]2+, Sens. Actuators B Chem. 252 (2017) 313–321, https://doi.org/10.1016/j.snb.2017.05.164.
[29] J.C. Ellerbrock, S.M. McLoughlin, A.I. Baba, The effect of pH on the emission and absorption spectra of a ruthenium complex, Inorg. Chem. Commun. 5 (2002) 555–559, https://doi.org/10.1016/S1387-7003(02)00480-X.
[30] E.M. Ryan, R. Wang, J.G. Vos, R. Hage, J.G. Haasnoot, The effect of the nature of the polypyridyl ligand on the physical properties of ruthenium polypyridyl compounds containing pyridyltriazoles, Inorg. Chim. Acta 208 (1993) 49–58, https://doi.org/10.1016/S0020-1693(00)82883-2.
[31] M.D. Marazuela, M.C. Moreno Bondi, G. Orellana, Enhanced performance of a fibre-optic luminescence CO2 sensor using carbonic anhydrase, Sens. Actuators B Chem. 29 (1995) 126–131, https://doi.org/10.1016/0925-4005(95)01673-2.
[32] I. Urriza-Arsuaga, M. Bedoya, G. Orellana, Tailored luminescent sensing of NH3 in biomethane productions, Sens. Actuators B Chem. 292 (2019) 210–216, https://doi.org/10.1016/j.snb.2019.04.109.
[33] A dye may also be a genuine pH indicator dye, even if there is no established equilibrium in the excited state, as long as the two species do not start equilibrating within their excited state lifetime. In this case, the contribution of each species (acidic and basic) is solely defined by the ground state pH equilibrium. Another possibility is the spectral separation of the acidic and basic species, where the two forms are either excited or emit at different wavelengths., (n.d.).
[34] M.G. Orellana, G.M. Bedoya, Luminescent ruthenium (II) complexes and their use in pH sensors, WO2016071465A1 (2016).
[35] C. Sawatari, T. Yagi, Introduction of amino groups into cellulose via (2, 3-Dibromopropyl) cellulose under mild conditions, Seni Gakkaishi 47 (1991) 467–475, https://doi.org/10.2115/fiber.47.9_467.
[36] J.W. Park, J. Ahn, C. Lee, Dependence of the photophysical and photochemical properties of the photosensitizer tris(4,4′-dicarboxy-2,2′-bipyridine)ruthenium(II) on pH, J. Photochem. Photobiol. Chem. 86 (1995) 89–95, https://doi.org/10.1016/1010-6030(94)03928-N.
[37] M.K. Nazeeruddin, K. Kalyanasundaram, Acid-base behavior in the ground and excited states of ruthenium(II) complexes containing tetraimines or dicarboxybipyridines as protonatable ligands, Inorg. Chem. 28 (1989) 4251–4259, https://doi.org/10.1021/ic00322a015.
[38] Z. Murtaza, Q. Chang, G. Rao, H. Lin, J.R. Lakowicz, Long-lifetime metal–ligand pH orobe, Anal. Biochem. 247 (1997) 216–222, https://doi.org/10.1006/abio.1997.2057.
[39] W. Xu, J. Mehlmann, J. Rice, J.E. Collins, C.L. Fraser, J.N. Demas, B.A.D. Jr, M. Bassetti, pH Sensors Based on Luminescent Ruthenium(II) Alpha-Diimine Complexes with Diethylaminomethyl Sensing Groups. in: Environ. Monit. Remediat. Technol., SPIE, 1999, pp. 456–465, https://doi.org/10.1117/12.339027.
[40] Corwin Hansch, A. Leo, R.W. Taft, A survey of Hammett substituent constants and resonance and field parameters, Chem. Rev. 91 (1991) 165–195, https://doi.org/10.1021/cr00002a004.
[41] C. Malins, H.G. Glever, T.E. Keyes, J.G. Vos, W.J. Dressick, B.D. MacCraith, Sol–gel immobilised Ruthenium(II) polypyridyl complexes as chemical transducers for optical pH sensing, Sens. Actuators B Chem. 67 (2000) 89–95, https://doi.org/10.1016/S0925-4005(00)00411-1.
[42] S. Lee, B.L. Ibey, G.L. Coté, M.V. Pishko, Measurement of pH and dissolved oxygen within cell culture media using a hydrogel microarray sensor, Sens. Actuators B Chem. 128 (2008) 388–398, https://doi.org/10.1016/j.snb.2007.06.027.
[43] C.-M. Chan, K.-Y. Wong, Evaluation of a luminescent Ruthenium complex immobilized inside nafion as optical pH sensor, Analyst 123 (1998) 1843–1847, https://doi.org/10.1039/A802460J.
[44] J.M. Price, W. Xu, J.N. Demas, B.A. DeGraff, Polymer-supported pH sensors based on hydrophobically bound luminescent Ruthenium(II) complexes, Anal. Chem. 70 (1998) 265–270, https://doi.org/10.1021/ac9707848.
[45] I. Urriza-Arsuaga, M. Bedoya, G. Orellana, Luminescent sensor for O2 detection in biomethane streams, Sens. Actuators B Chem. 279 (2019) 458–465, https://doi.org/10.1016/j.snb.2018.09.108.
[46] J. Gong, M.G. Tanner, S. Venkateswaran, J.M. Stone, Y. Zhang, M. Bradley, A hydrogel-based optical fibre fluorescent pH sensor for observing lung tumor tissue acidity, Anal. Chim. Acta 1134 (2020) 136–143, https://doi.org/10.1016/j.aca.2020.07.063.
[47] C.G. Frankær, K.J. Hussain, T.C. Dörge, T.J. Sørensen, Optical chemical sensor using intensity ratiometric fluorescence signals for fast and reliable pH determination, ACS Sens 4 (2019) 26–31, https://doi.org/10.1021/acssensors.8b01485.
[48] W.-H. Chen, W.D.N. Dillon, E.A. Armstrong, S.C. Moratti, C.M. McGraw, Self-referencing optical fiber pH sensor for marine microenvironments, Talanta 225 (2021) 121969, https://doi.org/10.1016/j.talanta.2020.121969.
[49] J. Werner, M. Belz, K.-F. Klein, T. Sun, K.T.V. Grattan, Fiber optic sensor designs and luminescence-based methods for the detection of oxygen and pH measurement, Measurement 178 (2021) 109323, https://doi.org/10.1016/j.measurement.2021.109323.
[50] N. Bustamante, G. Ielasi, M. Bedoya, G. Orellana, Optimization of temperature sensing with polymer-embedded luminescent Ru(II) complexes, Polymers 10 (2018) 234, https://doi.org/10.3390/polym10030234.
[51] M.D. Marazuela, M.C. Moreno-Bondi, G. Orellana, Luminescence lifetime quenching of a Ruthenium(II) Polypyridyl dye for optical sensing of carbon dioxide, Appl. Spectrosc. 52 (1998) 1314–1320, https://doi.org/10.1366/0003702981942825.
[52] Guillermo Orellana, M.C. Moreno-Bondi, Eva Segovia, M.D. Marazuela, Fiber-optic sensing of carbon dioxide based on excited-state proton transfer to a luminescent Ruthenium(II) complex, Anal. Chem. 64 (1992) 2210–2215, https://doi.org/10.1021/ac00043a005.

Ya Jie Knöbl received her BSc degree in Chemistry from the University of Graz in Austria in 2017. During her studies she became fascinated with photochemistry and completed several internships in the optical sensors laboratory to gain experience and knowledge. Later, she continued her studies at the Technical University of Graz and obtained her Master of Science degree in 2019 with a thesis on polymeric materials exhibiting thermally activated delayed fluorescence. Seeking to broaden her horizons, she accepted a PhD position in Prof. Orellana group at Complutense University of Madrid, Spain. There she was assigned to research luminescence lifetime-based sensors.

Maximino Bedoya received his BSc degree in Analytical Chemistry from UCM, followed by a PhD degree in the same discipline under the supervision of Prof. M. C. Moreno-Bondi, a "sandwich" doctorate splitting his academic research with industrial work on the applications of his luminescent optochemical sensors. After a short postdoctoral stage with Prof. Orellana at UCM, he was hired as R+D specialist by the Spanish company Interlab to develop novel fiber-optic chemical sensors and the associated optoelectronic instrumentation for environmental, industrial and aeronautic applications, some of them as Project Leader. In 2013 he returned to Prof. Orellana GSOLFA Group at UCM as Senior Researcher to carry out contract research on advanced luminescent chemosensors funded by multinational industrial leaders in bioreactor manufacturing, solar thermal power plants, gas distribution, and power generation, among others.

Alexander Farquharson was an Erasmus student at UCM for 6 months from Durham University in the UK. After completing his degree and Master of Chemistry there, he did a Master of Data Science at the University of Bristol. He is currently a data scientist at Cotiviti in Sydney(Australia).

Patrick Courtney has 20 years industrial experience in technology development and worked as Director for global firms such as PerkinElmer, as well as at Sartorius and Cap Gemini. He co-leads a European working group on analytical laboratory robotics and is member of board of directors of SiLA (Standards in Laboratory Automation). He holds an

MBA with a PhD in Robotic Engineering/Molecular Biology, has 100 publications and is named on ten patents.

Guillermo Orellana, Full Professor of Organic Chemistry and Photochemistry at Complutense University of Madrid (UCM) in Spain, received his PhD in Chemistry from the same University and was a Fulbright Postdoctoral Scholar at Columbia University in the City of New York in Prof. Turro group. He leads the multidisciplinary UCM Optical Chemosensors & Applied Photochemistry Group (GSOLFA). His research interests include novel photochemical principles for optical chemical sensing, molecular engineering of indicator dyes, molecular recognition (nano)materials, fiber-optic chemical sensors and biosensors and optoelectronic instrumentation for environmental monitoring, (bio)process analysis, and aerospace. He boasts a long-standing collaboration with industrial partners and the transfer of research results through agreements, authoring many international and national patents.